

Evidence for Kondo Effect in $\text{Au}_{80}\text{Co}_{20}$ Ribbons

D.S. Geoghegan,* A. Hütten, K.-H. Müller, and L. Schultz

IFW Dresden, Helmholtzstraße 20, D-01069 Dresden, Germany

(3 March 1997)

Abstract

A minimum in resistivity as a function of temperature for an as-quenched $\text{Au}_{80}\text{Co}_{20}$ ribbon prepared by melt-spinning using a wheel surface speed of 20 m s^{-1} is found at 25 K. No resistivity minimum is found for an as-quenched ribbon using a wheel surface speed of 60 m s^{-1} , however, upon heat treatment of this ribbon a resistivity minimum is recovered. The temperature of the minimum decreases with increasing total time of heat treatment. These observations are interpreted as evidence for the microstructural control of the Kondo effect typically found in dilute magnetic alloys in a giant magnetoresistance granular material.

72.15.Eb, 72.15.Qm 72.15.Gd, 75.70.Pa,

Typeset using REVTeX

*If you have read this paper and wish to be included in a mailing list (or other means of communication) that I maintain on the subject, then send e-mail to: seang@ifw-dresden.de

Giant magnetoresistance (GMR) is one mechanism controlling the magnetic field dependence of resistivity, ρ , of a material in which spin dependent scattering occurs within the bulk of, and at interfaces separating, non-magnetizable (NM) and magnetizable (M) regions. GMR was first observed in a multilayer (ML) of Fe/Cr¹ and later in granular materials.^{2,3} Among the models used to describe GMR and magnetization in these materials are models based on superparamagnetism (SPM).⁴⁻⁷ The SPM models do not adequately describe the low temperature and high field behaviour of ultra-fine M entities dispersed in a conducting NM matrix. To explain this discrepancy, an almost two orders of magnitude increase in the magnetocrystalline anisotropy energy density has been used⁵ although equally possible is that the average magnetic moment per M ion is reduced, as has been observed in Au-Co granular GMR ribbons.⁸

The Kondo effect⁹ results in a reduction of the effective magnetic moment of individual M ions due to localization of conduction electrons of opposite spin. It has been reported that evidence of Kondo scattering at low temperatures can be found in Au-Fe GMR materials.^{10,11} Since most NM-M alloys used at the basis for GMR materials exhibit Kondo scattering in the dilute limit¹² and local concentrations of M ions in the NM matrix may be below the concentration limit for the Kondo effect to occur (M ion concentrations typically < 0.1 at%), the expectation of a reduction in average M ion magnetic moment in GMR materials is not unreasonable. There are three identifiers of the Kondo effect: (i) a minimum in ρ below the Kondo temperature, T_K , below which $\rho \propto -\ln(T)$, (ii) a specific heat singularity at T_K , and (iii) a reduction in the M ion magnetic moment identifiable through magnetic susceptibility measurements in which the Curie-Weiss law is not followed.

The Au-Co binary alloy shows eutectic decomposition at Au_{75.1}Co_{24.9} and $T = 996.5^\circ\text{C}$. Hütten *et al.*⁸ estimated the upper limit of the chemical and coherent spinodals for Au-Co. Using these calculations, alloys of Au₈₀Co₂₀ should decompose via a eutectic decomposition rather than following a spinodal mechanism when heat treated at 400°C . The solubility of Co in Au below 422°C is very limited and much smaller than 0.2 at%¹³ hence a Au-Co alloy heat treated at 400°C should decompose into essentially pure Au and Co. Microstructural

studies of rapidly quenched Au–Co alloys^{8,14,15} have found that, for Co concentraions greater than 15 at%, Au–rich grains are found in the as–quenched state, the boundaries of which are decorated with heterogeneously formed spherical fcc essentially pure Co precipitates with diameters of up to 100 nm. The grain interiors are characterised by a lamellae eutectic consisting of Co–rich lamellae separated by Au–rich lamellae. Annealing at 480°C dissolves the eutectic and large essentially pure Co precipitates are formed at the grain boundaries and within the grains through the transfer of Co ions from the Au–rich lamellae to the Co–rich lamellae and finally to the Co precipitates using the Co–rich lamellae as diffusion paths.¹⁴

Two ingots of Au₈₀Co₂₀ were prepared by arc melting elemental components of greater than 99.9% purity in a high purity Ar atmosphere of 20 kPa to yield a total mass of 2.5 to 3 g per ingot. The weight loss during arc melting was less than 2%. Melt–spinning was performed by ejection of the molten alloy through a 0.6 mm diameter round hole perforating the bottom of a quartz crucible, with an ejection pressure of 20 kPa and 60 kPa, onto a rotating lightly sanded Cu wheel, with a wheel surface speed, v_s , of 20 m s^{−1} and 60 m s^{−1}, respectively. A chamber pressure of less than 10^{−3} Pa was established prior to ejection of the melt and the height of the crucible above the surface of the Cu wheel was 0.40 ± 0.05 mm. Typical ribbon pieces had lengths of 2 to 30 cm, widths of 0.5 to 1 mm and thicknesses of 20 to 40 μm.

Heat treament of the ribbon quenched using $v_s = 60$ m s^{−1} was conducted at 400°C in a closed quartz tube containing 10 kPa high purity Ar with the samples contained in Ta boats. The total time of heat treatment, t_{ann} , ranged from 10 min to 4 h with quenching to room temperature by immersion of the annealing tube in water at intermediate times to retrieve samples at different stages of heat treatment. The composition of all samples was determined by microprobe analysis which found the samples to have a composition within ±0.2 at% of the nominal composition.

Measurements of longitudinal MR (L–MR, made with the external field, H_{ext} , parallel to the drive current, i) were made at temperatures from 10 K to 300 K in magnetic fields

of up to 5 T in a Lakeshore 7225 susceptometer with the resistance option and of L-MR and transverse MR (T-MR, made with H_{ext} perpendicular to i) in magnetic fields of up to 7 T in a split coil solenoid from Oxford Instruments. The resistance of the samples was measured by the four point contact method from which the MR ratio and ρ were calculated. Measurements of magnetization were performed using a SQUID magnetometer in magnetic fields of up to 4 T from 5 K to 300 K. Total AC susceptibility, χ_{tot} was measured in the Lakeshore 7225 susceptometer used for the resistivity measurements with an AC field magnitude of 2.5 mT at a frequency of 133 Hz. Differential scanning calorimetry (DSC) measurements were performed from 93 K to 673 K on a TA Instruments DSC 2910.

The MR ratio, $\Delta\rho/\rho_0$, is defined in this work as $\Delta\rho/\rho_0 = [\rho(H_{ext}) - \rho(0)]/\rho(0)$ where $\rho(H_{ext})$ is the resistivity for an external field equal to H_{ext} . $\rho(H_{ext})$ is measured at a series of H_{ext} values corresponding to a full hysteresis loop (i.e. measurements from $H_{ext} = 0 \rightarrow H_{max} \rightarrow -H_{max} \rightarrow 0$ where H_{max} is the maximum external field possible with the measurement device) after exposing the samples to the maximum reverse field.

The temperature dependence of χ_{tot} of the as-quenched samples shows a small peak at about 10 K superimposed on a generally constant larger value and the field cooled (FC) magnetization curve separates from the zero field cooled (ZFC) magnetization curve just below room temperature. These results are consistent with spin-glass (SG) behaviour (as was concluded by Kataoka *et al.*¹⁵ for an aged $\text{Au}_{85}\text{Co}_{15}$ foil) as well as SPM. A distinction between either is difficult to establish without a knowledge of the microstructure of the Co in the Au-rich lamellae and Au-matrix grains. Although χ_{tot} does not follow Curie-Weiss behaviour, it is difficult to attribute this to the Kondo effect. The observation of both a peak in χ_{tot} and splitting of the FC and ZFC magnetization curves, indicating the presence of either or both of a SG and SPM particles, is not surprising given the complex nature of the microstructure. DSC measurements do not show any specific heat singularity that can be associated with a Kondo temperature.

In Fig. 1 is shown L-MR, expressed as a MR ratio, as a function of $\mu_0 H_{ext}$, reduced magnetization, M/M_{max} , as a function of $\mu_0 H_{ext}$, and L-MR as a function of M/M_{max} , all

measured at 10 K, for $\text{Au}_{80}\text{Co}_{20}$ ribbon ($v_s = 60 \text{ m s}^{-1}$) heat treated at 400°C for a total time of 40 min. M_{max} measured at 4 T is $9.94 \text{ A m}^2/\text{kg}$ which is 82% of the value expected assuming simple dilution of magnetization by the Au, similar to the result obtained by Hütten *et al.*⁸ Measurement of T-MR shows significant anisotropic MR (AMR) which is due to ferromagnetic-like regions in the ribbon, the full results of these will be presented elsewhere.¹⁶ The low field GMR is ML-like (i.e. proportional to the square of magnetization and saturating in low fields) and at high fields the magnetization and the GMR increases almost linearly with H_{ext} consistent with the arguments of Wiser⁷ concerning scattering between SPM and blocked M entities in the material.

Shown in Fig. 2 is ρ of as-quenched $\text{Au}_{80}\text{Co}_{20}$ ribbon ($v_s = 20 \text{ m s}^{-1}$) as a function of temperature for constant external magnetic fields. The linear increase in ρ with the decrease in the logarithm of temperature below $T = 25 \text{ K}$ for $H_{ext} = 0$ suggests that at least some of the Co is diluted enough in the Au-rich lamellae and/or Au-matrix grains for the Kondo effect to occur. Kondo scattering at these temperatures results in an extra magnetic contribution to ρ and an enhancement of the measured GMR response as can be seen from the splitting of the ρ curves measured at the different values of external magnetic field. Any SG regions would also contribute towards the enhancement in GMR at these temperatures.

In Fig. 3 is shown the development of ρ as a function of temperature for $\text{Au}_{80}\text{Co}_{20}$ ribbon ($v_s = 60 \text{ m s}^{-1}$) heat treated at 400°C for a total time of: (a) 0 min (as-quenched), (b) 10 min, (c) 40 min, and (d) 4 h. In addition to the general decrease in ρ with heat treatment, minima in ρ can be found for the heat treated ribbons, the temperature of which decreases with increasing t_{ann} . The development of the temperature dependence of ρ with t_{ann} is not consistent with an increase of a contribution from the Kondo effect since: (i) one would naturally assume that a decrease of the Co concentration in the Au-rich lamellae and/or Au-matrix grains from a increase in t_{ann} would result in an increase in the effective Kondo temperature, and (ii) these results are consistent with the interpretation that the minima in ρ are associated with SG transition temperatures since the temperature of the SG transition should decrease with decreasing Co concentration in the Au-rich lamellae and/or Au-matrix

grains. However the increase in ρ with the logarithm of temperature as the temperature decreases as shown in Fig. 2 as well as the preceding minimum in ρ are indicative of the Kondo effect since the M ion magnetic moment correlation length in a SG monotonously increases with decreasing temperature until the spin freezing temperature is reached where upon it remains almost constant.

In conclusion, we have observed in $\text{Au}_{80}\text{Co}_{20}$ ribbons prepared by melt-spinning and subsequent heat treatment resistivity minima associated with the Kondo effect. It is possible that the reduction of the M ion magnetic moment in GMR materials due to the Kondo effect can explain the difficulty in fitting the observed magnetic properties to the proposed SPM models and avoid the almost two orders of magnitude increase in magnetocrystalline anisotropy energy density⁵ particularly if the Kondo effect results in significant reduction in the effective magnetic moment of the M ions contributing to the magnetic and resistivity changes at high fields in these materials. Determination of the Co concentrations in the Au-rich lamellae would confirm these conclusions which is expected to be accomplished soon.

We would like to thank Dr. B. Idziwowski for discussions, Dr. D. Eckert for performing the magnetization measurements, and H. Schuffenhauer for performing the microprobe analysis.

REFERENCES

- ¹ M.N. Baibich, J.M. Broto, A. Fert, F. Nguyen Van Dau, F. Petroff, P. Etienne, G. Creuzet, A. Friederich, and J. Chazelas, Phys. Rev. Lett. **61** 2472 (1988).
- ² A.E. Berkowitz, J.R. Mitchell, M.J. Carey, A.P. Young, S. Zhang, F.E. Spada, F.T. Parker, A. Hütten, and G. Thomas, Phys. Rev. Lett. **68** 3745 (1992).
- ³ J.Q. Xiao, J.S. Jiang, and C.L. Chien, Phys. Rev. Lett. **68** 3749 (1992).
- ⁴ S. Zhang, and P.M. Levy, J. Appl. Phys. **73** 5315 (1993).
- ⁵ B.J. Hickey, M.A. Howson, D. Greig, and N. Wiser, Phys. Rev. B **53** 32 (1996).
- ⁶ T. Luciński, D. Elefant, G. Reiss, and P. Verges, JMMM **162** 29 (1996).
- ⁷ N. Wiser, JMMM **159** 119 (1996).
- ⁸ A. Hütten, J. Bernardi, S. Friedrichs, G. Thomas, and L. Balcells, Scripta Met. Mat. **33** 1647 (1995).
- ⁹ J. Kondo, *Theory of dilute magnetic alloys*, in Solid State Physics, (F. Seitz, D. Turnbull, and H. Ehrenresch, eds.) Academic Press, New York 183 (1969).
- ¹⁰ H. Sato, Y. Kobayashi, Y. Aoki, K. Shintaku, N. Hosoi, and T. Shinjo, J. Phys. Soc. Jap. **62** 3380 (1993).
- ¹¹ N. Giordano, Phys. Rev. B **53** 2487 (1996).
- ¹² P.L. Rossiter, and J. Bass, *Electronic transport properties of normal metals*, in Materials Science and Technology (ed. K.H.J. Buschow), VCH Publishers Inc., **3A** (1992).
- ¹³ H. Okamoto, T.B. Massalski, M. Hasebe, and T. Nishizawa, Bull. Alloy Phase Diag. **6** 449 (1985).
- ¹⁴ J. Bernardi, A. Hütten, S. Friedrichs, C.E. Echer, and G. Thomas, Phys. Stat. Solidi (a) **147** 165 (1995).

- ¹⁵ N. Kataoka, H. Takeda, J. Echigoya, K. Hukamichi, E. Aoyagi, Y. Shimada, H. Okuda, K. Osamura, M. Furusaka, and T. Goto, JMMM **140–144** 621 (1995).
- ¹⁶ D.S. Geoghegan, A. Hütten, G. Schmitz, K.–H. Müller, and L. Schultz, International Conference on Magnetism 1997 (submitted).

FIGURES

FIG. 1. (a) L-MR, expressed as a MR ratio, as a function of $\mu_0 H_{ext}$, (b) reduced magnetization, M/M_{max} , as a function of $\mu_0 H_{ext}$, and (c) L-MR as a function of M/M_{max} , for $\text{Au}_{80}\text{Co}_{20}$ ribbon, melt-spun using $v_s = 60 \text{ ms}^{-1}$ and heat treated at 400°C for a total time of 40 min, measured at $T = 10 \text{ K}$.

FIG. 2. Resistivity, ρ , as a function of temperature for as-quenched $\text{Au}_{80}\text{Co}_{20}$ ribbon, melt-spun using $v_s = 20 \text{ ms}^{-1}$, in constant external magnetic fields. A minimum in ρ at $T = 25 \text{ K}$ and below this minimum $\rho \propto -\ln(T)$ for $H_{ext} = 0$.

FIG. 3. Resistivity, ρ , as a function of temperature for $\text{Au}_{80}\text{Co}_{20}$ ribbon, melt-spun using $v_s = 60 \text{ ms}^{-1}$ and heat treated at 400°C for a total time of: (a) 0 min (as-quenched), (b) 10 min, (c) 40 min, and (d) 4 h. Resistivity minima are only found for heat treated ribbons, which occur at: (b) 14 K, (c) 12 K, and (d) 11 K. Note the change of scale for each curve.

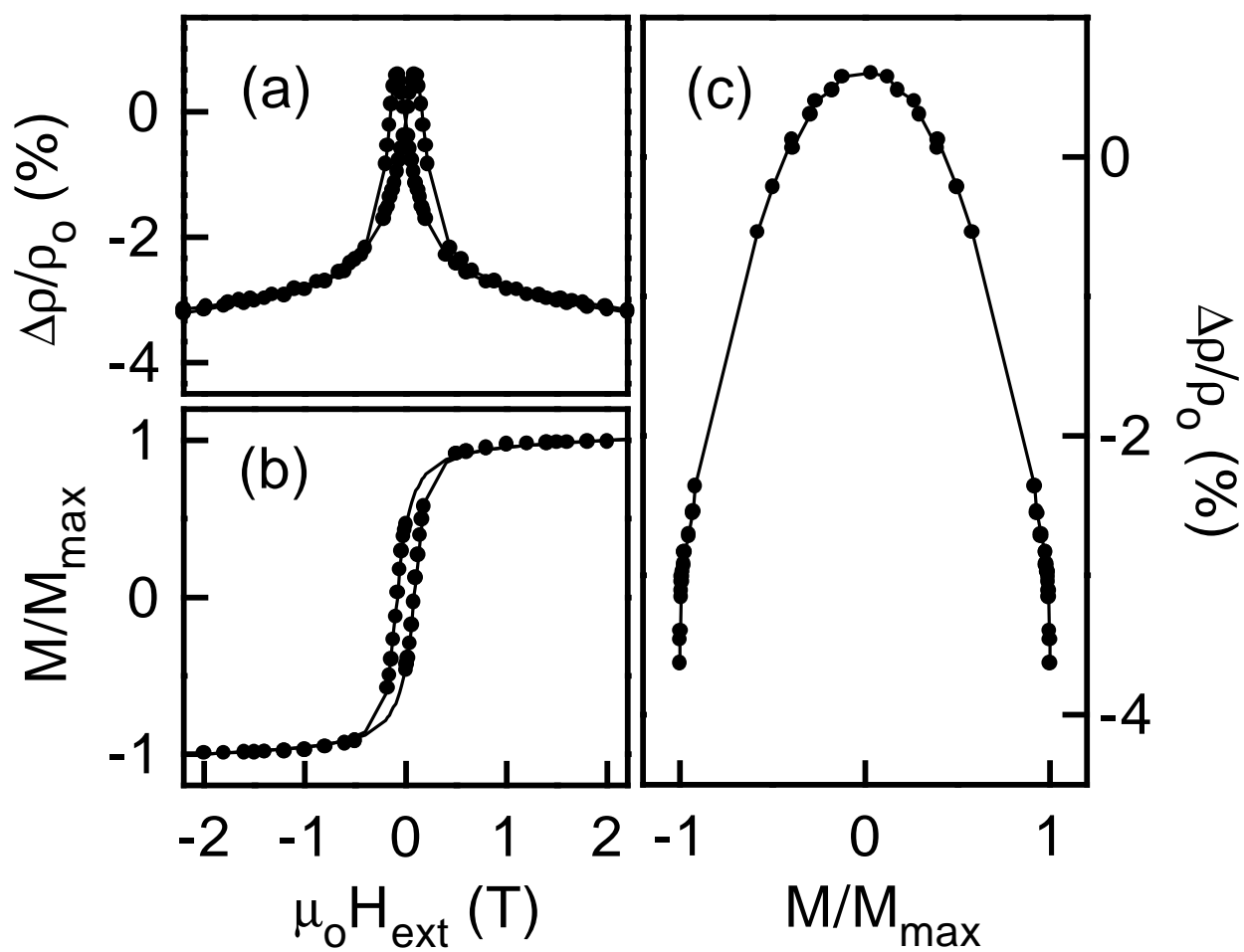


Fig. 1

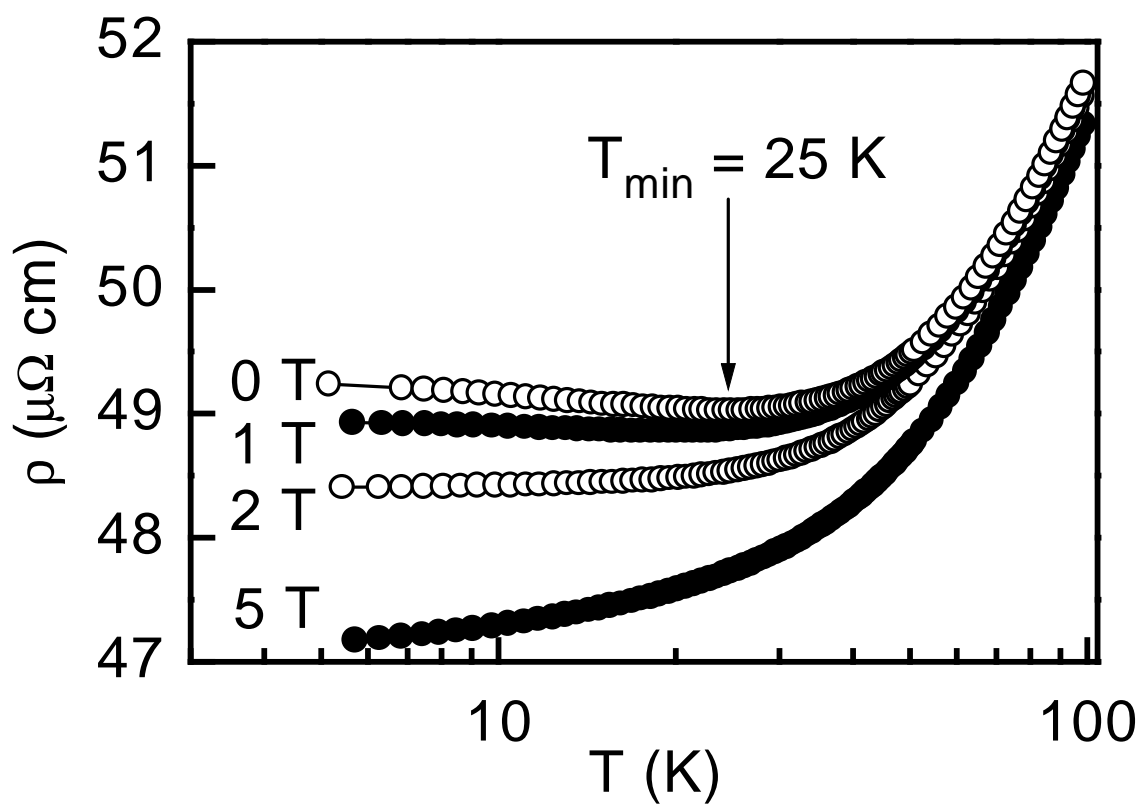


Fig. 2

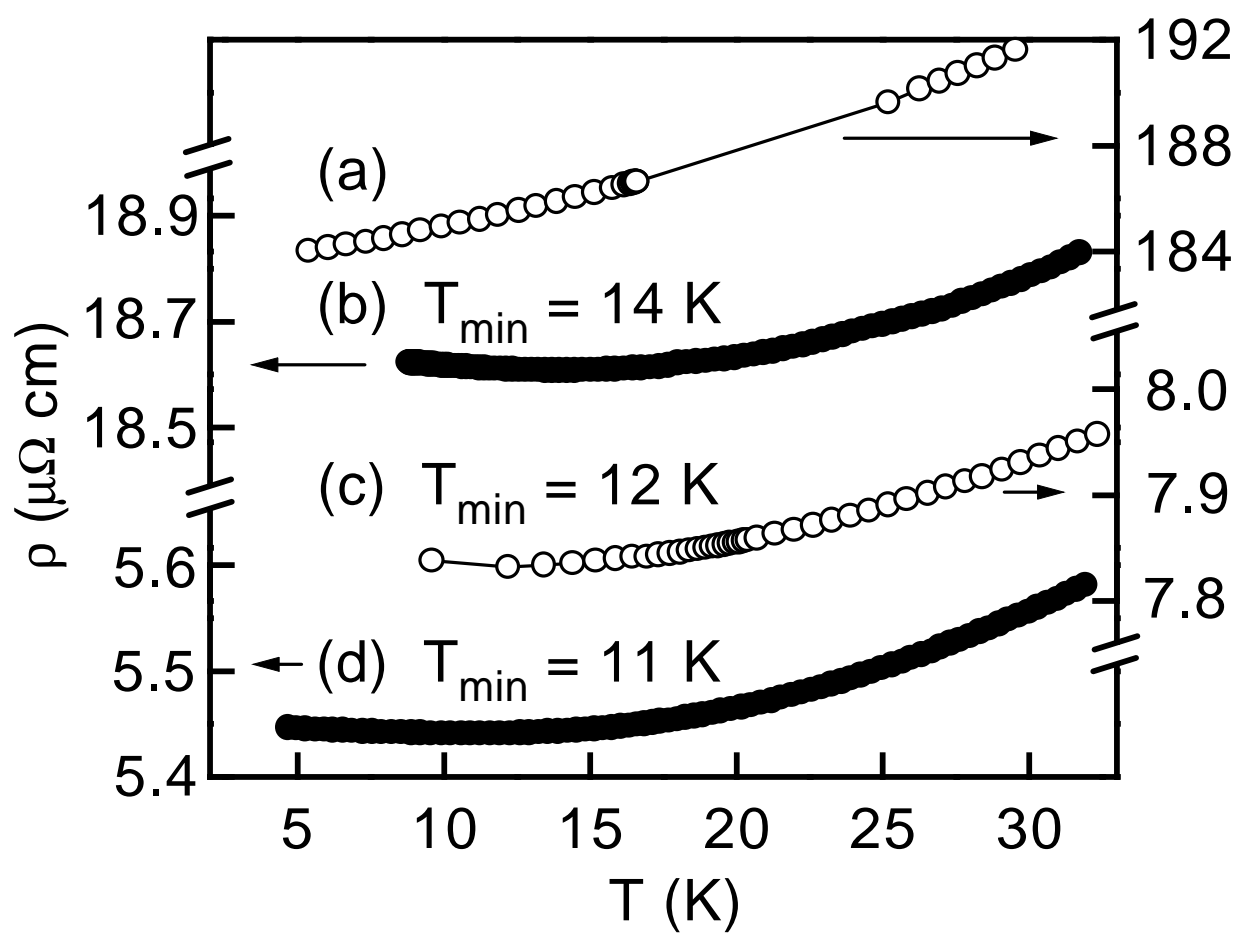


Fig. 3